

## An optimization-based model of iron–light–ammonium colimitation of nitrate uptake and phytoplankton growth

Robert A. Armstrong

Program in Atmospheric and Oceanic Sciences, Sayre Hall, P.O. Box CN710, Princeton University, Princeton, New Jersey 08544

### Abstract

The ability to model “new” (nitrate-based) production is crucial to predicting the ocean’s role in the global carbon cycle. The ability to model the distribution of high-nutrient/low-chlorophyll (HNLC) areas is particularly important in this regard. Here I draw together three elements that appear to be necessary for constructing the required model: (1) iron limitation of algal growth rates as an ultimate cause of the HNLC condition; (2) ammonium inhibition of nitrate uptake and utilization as a proximate mechanism that leads to reduced nitrate use; and (3) the dependence of both processes on algal cell size. In the model, cells are postulated to maximize their growth rates by partitioning scarce iron between nitrogen- and carbon-related demands. The effect of iron limitation is postulated to depend on cell size through surface/volume effects on uptake efficiency; this dependence on cell size in turn affects phytoplankton community structure and community-level uptake of nitrate. The efficacy of the model is demonstrated by its ability to reproduce community-level curves of nitrate uptake versus ammonium concentration from both HNLC and non-HNLC areas. The partition formalism can be incorporated directly into ecosystem models; when implemented in an ecosystem model with multiple size classes, the model should produce HNLC versus non-HNLC conditions in appropriate locations and for appropriate reasons. In particular, the model’s ability to produce iron–light and iron–light–nitrogen colimitation should be useful in understanding and predicting the HNLC condition in parts of the Southern Ocean. With suitable changes to parameter values, the postulated mechanism for iron partitioning may also prove useful in modeling iron and energy partitioning in nitrogen fixers.

The ability to model the distribution of high-nutrient/low-chlorophyll (HNLC) areas, where concentrations of nitrate and phosphate remain high throughout the year, is critical to prognostic studies of the global carbon cycle. Empirical evidence suggests that the ability to model iron limitation of growth and nitrate uptake will be a key element in predicting HNLC conditions. As the prime example, a scarcity of iron has recently been shown to limit phytoplankton growth, biomass accumulation, and size and taxonomic structure in the equatorial Pacific, a major HNLC region (Coale et al. 1996). Addition of iron to surface waters of this region caused a massive phytoplankton bloom and drawdown of nitrate, accompanied by a marked reduction in the fugacity of CO<sub>2</sub> (Cooper et al. 1996). The possibility of similar conversion of the subarctic Pacific (La Roche et al. 1996) and the Southern Ocean (de Baar et al. 1995; Kumar et al. 1995) from HNLC to non-HNLC by the addition of iron is supported by more indirect evidence.

### Acknowledgments

Conversations with Richard Geider helped greatly in the development of these ideas, particularly in the realization that it could be extremely useful scientifically to have a single model of iron limitation that both biogeochemists and physiologists could discuss and improve. I thank Rick Murnane, Jorge Sarmiento, Bess Ward, and Cindy Lee for helpful comments on the manuscript. Comments and suggestions by the editor, David Kirchman, were especially valuable in improving the presentation.

The support of National Science Foundation grants OCE 93-14707 and OCE 97-12204, National Aeronautics and Space Administration grant NAGW-3137, National Oceanic and Atmospheric Administration grant NA56GP0439, and U.S. Department of Energy grant DE-FG02-90ER61052 to J.L. Sarmiento are gratefully acknowledged.

The mechanistic basis of the HNLC pattern in the equatorial Pacific is thought to involve an interaction between grazing and iron limitation. In this scenario, resident (small-celled) populations are kept in check by the grazing of microzooplankton (Banse 1990; Miller et al. 1991; Coale et al. 1996; Landry et al. 1997). Larger phytoplankton species are thought to be more susceptible to iron limitation because of their smaller surface/volume ratios (Hudson and Morel 1990; Morel et al. 1991; Price et al. 1991; Sunda and Huntsman 1997). Large phytoplankton are also thought to be controlled at low densities by the grazing of large, generalized grazers, such as copepods, whose populations are sustained by their ability to graze on smaller phytoplankton and zooplankton size classes. The result is a system in which size classes (particularly smaller size classes) are each limited by predation (i.e., they are controlled “top down”), whereas total phytoplankton biomass is controlled through the scarcity of iron (“bottom-up” control), leading to “grazer-controlled phytoplankton populations in an iron-limited ecosystem” (Price et al. 1994; *see also* Armstrong 1994 and Landry et al. 1997).

Observed relationships between nitrate uptake and ammonium concentration are quite variable (Fig. 1). Wheeler and Kokkinakis (1990) hypothesized that this variability falls into two broad classes. The more usual curve is roughly hyperbolic, with nitrate uptake declining asymptotically to zero with increasing ammonium concentration. In the subarctic Pacific and certain other regions, however, uptake appears to decline almost linearly with ammonium concentration.

The working hypothesis of this article is that these differences are mechanistically related to the availability of iron, because the areas cited by Wheeler and Kokkinakis

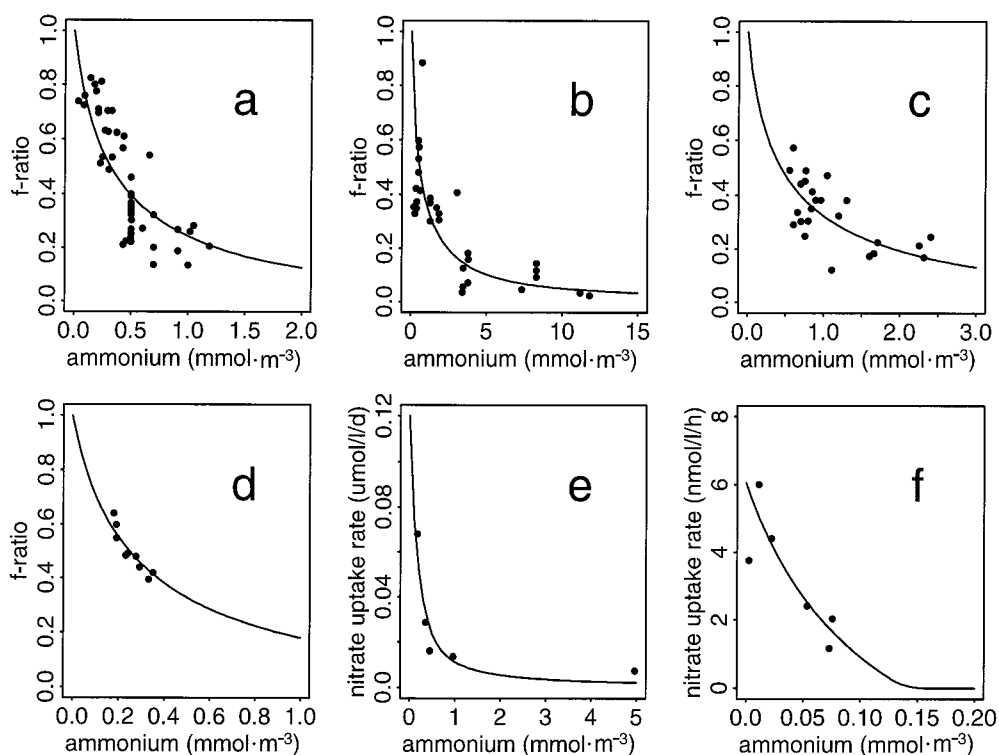


Fig. 1. Data fits of the model to six data sets: (a) Cochlan (1986), (b) Garside (1981), (c) Glibert et al. (1982), (d) Olson (1980), (e) Price et al. (1994), (f) Wheeler and Kokkinakis (1990).

(1990) as having straight-line relationships are HNLC regions. The model I have created to describe this situation predicts that when iron is abundant and cells are growing at near-maximal rates, nitrate use should approach zero asymptotically with increasing ammonium concentration; in contrast, the model predicts that when iron is scarce, the nitrate uptake curve should intersect the ammonium axis at a finite ammonium concentration, becoming almost linear in areas of severe iron stress.

The basic postulate of the model is that when iron is in short supply, iron limitation affects the ability of cells to acquire both carbon and nitrogen. An additional postulate is that through their evolutionary history, phytoplankton have developed mechanisms to partition scarce iron between carbon acquisition and nitrogen acquisition to maximize growth rate. The model is based on this optimality argument, and some physiological detail has been sacrificed to allow the optimality argument to be used. One important simplification is that carbon metabolism and nitrogen metabolism are treated as being independent, whereas recent empirically based model structures allow carbon acquisition to depend on cell nitrogen (Sciandra et al. 1997; Geider et al. 1998). Explicit modeling of physiological feedbacks between internal nitrogen stores and external ammonium and nitrate pools (Flynn et al. 1997) has also been suppressed for biogeochemical clarity. Nevertheless, the model structure provides a geochemically relevant framework within which new physiological results can be interpreted; it may therefore serve as a common meeting ground among physiologists, ecosystem modelers, and geochemists.

In the model, ammonium is the favored nitrogen source because it does not need to be reduced (Syrett 1981; Dortch 1990). When cells cannot satisfy their entire nitrogen requirement using ammonium, nitrate is taken up, and iron and reductant must be provided for nitrate reduction. Iron is partitioned between cell functions such that a certain fraction is allocated to nitrate reduction, and the remainder is reserved for cell functions related to carbon acquisition (part of which must be used to provide reductant for nitrate reduction). The partition fraction is altered dynamically to make the best use of limited iron and carbon to maximize phytoplankton growth rate; consequently, as ammonium concentration is increased, iron is shifted from nitrate reduction to energy-related cell functions.

Ideally, such a model should be formulated in terms of the full dynamics of nitrogen, carbon, and iron use within cells. Fully dynamic approaches to carbon and nitrogen cycling have recently been proposed (Flynn et al. 1997; Sciandra et al. 1997; Geider et al. 1998), and Flynn (pers. comm.) has proposed a detailed mechanistic model for iron that is similar in concept to the model in this article. However, in the interest of biogeochemical simplicity, I have taken a quasi-steady-state approach for carbon and nitrogen, because these elements cannot be stored in great excess (Morel 1987). This steady-state approximation for carbon and nitrogen is coupled to a fully dynamic description of iron cell quota, because iron can be stored in great excess (Morel 1987; Sunda and Huntsman 1995, 1997). Steady-state optimality arguments are then used to predict growth rates and

nitrate uptake rates as functions of iron cell quotas and ammonium uptake rates.

The resulting model allows cells to be colimited by iron, light, and nitrogen, so that if iron is scarce and there is not enough ammonium to supply the entire nitrogen requirement, cells will be colimited by light and nitrate reduction. Colimitation is not possible in models where iron is modeled as a direct limiting element (Loukos et al. 1997; Leonard et al. 1999) or where photosynthesis and nitrate reduction are modeled as being inhibited to equal degrees by lack of iron (Hurtt and Armstrong 1999). For example, the iron-limitation parameterization used by Hurtt and Armstrong (1999) predicted chronic light limitation in spring and summer at ocean weather station "India" (OWS I); this limitation was necessary to prevent complete uptake of nitrate during the growing season. In contrast, the present model would predict iron–light–nitrogen colimitation under the same circumstances.

After deriving the model, I discuss qualitatively how it can be used to produce nitrate uptake curves that are approximately straight-line functions of ammonium concentration under iron limitation while also producing curves that are hyperbolic when iron is abundant. Finally, I combine a linearized version of the model, which accords well with the data of Sunda and Huntsman (1997), with a model of algal size spectra (Hurtt and Armstrong 1996, 1999) to show that this combination can produce quantitatively the range of uptake curves shown in Fig. 1.

## Model

I begin with the Droop (1968) equation relating algal per capita growth rate  $\mu$  ( $\text{d}^{-1}$ ) to cell quota  $q$  (the amount of a specified nutrient per cell, with units  $\text{pmol cell}^{-1}$ ):

$$\mu = \mu'(1 - q_0/q). \quad (1)$$

In this expression,  $\mu' \equiv \mu_{\text{max}}/(1 - q_0/q_{\text{max}})$ , where  $q_0$  is the minimum cell quota and  $q_{\text{max}}$  is the maximum cell quota, so that  $\mu \rightarrow \mu_{\text{max}}$  as  $q \rightarrow q_{\text{max}}$ . In the Droop formulation, nutrient uptake parameters, cell quotas, and growth parameters are intimately related by the requirement that as steady state, a combination of Michaelis uptake kinetics with Droop dependence of growth rate on cell quota should yield Monod dependence of growth rate on extracellular nutrient concentration (Droop 1968; Goldman 1977; Burmaster 1979; Morel 1987). At steady state, uptake rates of nutrient per cell  $\rho$  are related to cell quota by  $q = \rho/\mu$  (Droop 1968); substituting this into Eq. 1 and rearranging as in Goldman (1977) yields

$$\mu = \mu'\rho/(\rho + \mu'q_0) \quad (2)$$

for  $\rho \leq \rho_{\text{max}} \equiv \mu_{\text{max}}q_{\text{max}}$ . Expressing growth as a function of uptake rates will prove useful in the nitrogen equation, where uptake rates of ammonium and nitrate must be summed.

I postulate that iron uptake is partitioned among cell functions to maximize growth rate (Fig. 2). I hypothesize that a fraction  $\eta$  of iron uptake is allocated to reducing nitrate and that this fraction determines the maximum flux of reduced nitrate,  $\rho_{\text{NO}_3, \text{red}}$ , that is available for growth. When added to the ammonium uptake rate,  $\rho_{\text{NH}_4}$ , which itself influences the optimal value of  $\eta$ , the flux of reduced nitrate,  $\rho_{\text{NO}_3, \text{red}}$ , de-

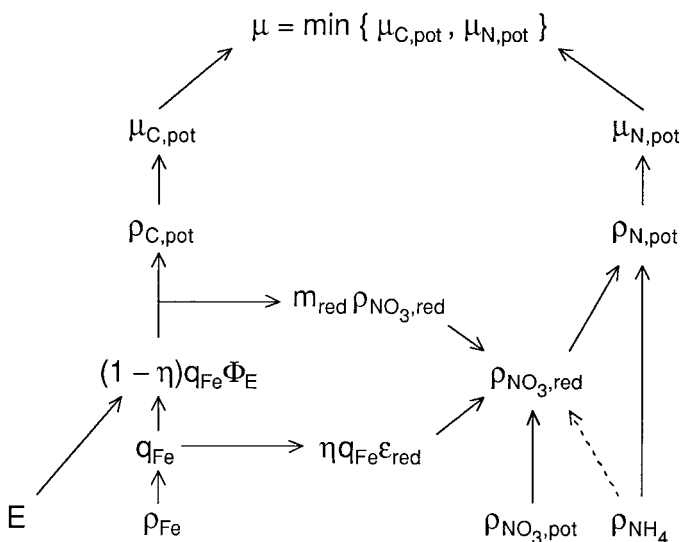


Fig. 2. Schematic flow diagram of the model (see text for details).

termines the potential nitrogen uptake rate,  $\rho_{\text{N,pot}}$ , and hence the potential nitrogen-limited growth rate,  $\mu_{\text{N,pot}}$ . I also hypothesize that a fraction  $1 - \eta$  of iron is reserved for energy (carbon)-related cell functions, including photosynthesis and electron transport, and that this fraction determines a potential carbon-limited growth rate,  $\mu_{\text{C,pot}}$ . Finally, I posit that  $\eta$  is dynamically altered to make the best use of limited iron by maximizing overall growth rate,  $\mu = \min\{\mu_{\text{C,pot}}, \mu_{\text{N,pot}}\}$ .

Mathematical forms for  $\mu_{\text{N,pot}}$  and  $\mu_{\text{C,pot}}$  must be specified as functions of iron availability. I will assume that the flux relevant to nitrogen limitation,  $\rho_{\text{N,pot}}$ , is the sum of a flux of reduced nitrate,  $\rho_{\text{NO}_3, \text{red}}$ , and an ammonium flux  $\rho_{\text{NH}_4}$ , although the model could be modified to include nitrate, urea, and other nitrogen sources. I also assume that the two iron fluxes needed for the model, for energy uptake and nitrate reduction, are each proportional to the amounts of iron that are allocated to these functions.

Potential uptake-limited rates of nutrient use for ammonium and nitrate are defined by the Michaelis uptake curves:

$$\rho_{\text{NH}_4, \text{pot}} = \rho_{\text{N,max}}[\text{NH}_4]/(K_{\text{NH}_4} + [\text{NH}_4]) \quad (3a)$$

and

$$\rho_{\text{NO}_3, \text{pot}} = \rho_{\text{N,max}}[\text{NO}_3]/(K_{\text{NO}_3} + [\text{NO}_3]). \quad (3b)$$

Ammonium will be taken up at its maximum potential rate if the potential carbon-limited growth rate,  $\rho_{\text{C,pot}}$ , is high enough; otherwise, ammonium will be taken up at some lower rate,  $\rho_{\text{NH}_4} < \rho_{\text{NH}_4, \text{pot}}$ .

If the demand for nitrogen is too large to be supplied by ammonium uptake alone, nitrate will be taken up subject to the constraint that the total nitrogen uptake rate must be less than the maximum allowable nitrogen uptake rate,  $\rho_{\text{N,max}}$ . Nitrate uptake is additionally constrained by the availability of iron for nitrate reduction. When nitrate is abundant, the flux of reduced nitrate,  $\rho_{\text{NO}_3, \text{red}}$ , is hypothesized to be proportional to the amount of iron per cell,  $\eta q_{\text{Fe}}$ , allocated to the nitrate reduction system, multiplied by an efficiency term,  $\epsilon_{\text{red}}$ , the rate of nitrate reduction that can be supported per unit iron.

Together these assumptions yield the potential rate (under nitrogen limitation) for nitrate uptake and reduction as

$$\rho_{\text{NO}_3,\text{red}} = \min\{\rho_{\text{NO}_3,\text{pot}}, \rho_{\text{N,max}} - \rho_{\text{NH}_4,\text{pot}}, \epsilon_{\text{red}}\eta q_{\text{Fe}}\}. \quad (4)$$

The potential total flux of nitrogen into the cell is then

$$\rho_{\text{N,pot}} = \rho_{\text{NO}_3,\text{red}} + \rho_{\text{NH}_4}, \quad (5)$$

yielding the potential nitrogen-limited growth rate,

$$\mu_{\text{N,pot}} = \mu'_{\text{N}}\rho_{\text{N,pot}}/(\rho_{\text{N,pot}} + \mu'_{\text{N}}q_{\text{N},0}). \quad (6)$$

In the Droop model, the relevant carbon flux is that which can contribute to an increase in the cell quota for carbon,  $q_{\text{C}}$ ; it is therefore the net flux of carbon once metabolic losses for maintenance and growth have been subtracted (Droop et al. 1982). Mathematically, the net flux of carbon (in excess of metabolic losses) is given by

$$\rho_{\text{C,pot}} = \epsilon_{\text{growth}}[(1 - \eta)q_{\text{Fe}}\Phi_{\text{E}} - m_{\text{bas}} - m_{\text{red}}\rho_{\text{NO}_3,\text{red}}] \quad (7a)$$

$$= \epsilon_{\text{growth}}[q_{\text{Fe}}\Phi_{\text{E}} - m_{\text{bas}} - (\Phi_{\text{E}}/\epsilon_{\text{red}} + m_{\text{red}})\rho_{\text{NO}_3,\text{red}}]. \quad (7b)$$

Here,  $\Phi_{\text{E}}$  is the rate of carbon fixation per unit of iron devoted to photosynthesis and related processes, so that  $(1 - \eta)q_{\text{Fe}}\Phi_{\text{E}}$  is the overall rate of carbon acquisition. The term  $m_{\text{red}}\rho_{\text{NO}_3,\text{red}}$  is the metabolic (carbon) cost associated with nitrate reduction;  $m_{\text{red}}$  is therefore the reductant required per unit of reduced nitrate. In addition, the term  $m_{\text{bas}}$  is a basal metabolic cost (assumed constant); if almost all metabolic cost can be associated with growth, this term will be nearly zero. Finally, the bracketed term, which represents the energy flux potentially available for growth, has been multiplied by an efficiency term,  $\epsilon_{\text{growth}}$ , to account for metabolic losses associated with growth. Note that there are two distinct carbon costs associated with nitrate reduction: a direct cost,  $m_{\text{red}}\rho_{\text{NO}_3,\text{red}}$ , for reductant, and an opportunity cost,  $\eta q_{\text{Fe}}\Phi_{\text{E}} = \rho_{\text{NO}_3,\text{red}}\Phi_{\text{E}}/\epsilon_{\text{red}}$ , for direct use of iron in the nitrate/nitrite reduction system. Both costs are proportional to  $\rho_{\text{NO}_3,\text{red}}$ , so even if the direct cost of using iron for enzymes and electron transport proteins in the nitrate/nitrite system is small relative to the cost of reductant, the balance between nitrogen limitation and carbon limitation will still be properly represented.

Equation 7 will be valid only up to some maximum value  $q_{\text{Fe}}^*$  for iron allocated to the carbon acquisition system, beyond which additional iron allocated to chlorophyll and photosynthetic electron transport gives no further increase in growth rate (Sunda and Huntsman 1997); Eq. 7 therefore holds only for  $(1 - \eta)q_{\text{Fe}} < q_{\text{Fe}}^*$ . (It would be mathematically convenient to ignore this limitation, but the experiments of Sunda and Huntsman (1997) clearly show that growth rate stops increasing well before the maximum cell quota of iron,  $q_{\text{Fe,max}}$ , is reached. This form of ‘‘luxury consumption’’ of iron is therefore quantitatively important and cannot be ignored.) The potential carbon-limited growth rate,  $\mu_{\text{C,pot}}$ , is then

$$\mu_{\text{C,pot}} = \mu'_{\text{C}}\rho_{\text{C,pot}}/(\rho_{\text{C,pot}} + \mu'_{\text{C}}q_{\text{C},0}). \quad (8)$$

Finally, to complete the model equations, we add a dynamic equation for iron quota,  $q_{\text{Fe}}$  (Droop 1968), that implicitly allows luxury consumption of iron:

$$dq_{\text{Fe}}/dt = \rho_{\text{Fe}} - \mu q_{\text{Fe}}. \quad (9)$$

## Regions of limitation and colimitation

Equations 3 through 9 define how the potential carbon-limited growth rate,  $\mu_{\text{C,pot}}$ , and the potential nitrogen-limited growth rate,  $\mu_{\text{N,pot}}$ , should depend on irradiance,  $E$ ; iron uptake rate,  $\rho_{\text{Fe}}$ ; ammonium uptake rate,  $\rho_{\text{NH}_4}$ ; and nitrate uptake rate,  $\rho_{\text{NO}_3,\text{pot}}$ . The next step is to find a value for the iron partition fraction that maximizes the realized algal growth rate,  $\mu = \min\{\mu_{\text{C,pot}}, \mu_{\text{N,pot}}\}$ .

Six cases must be defined. In cases where shortages of energy or iron cause limitation of nitrate reduction (cases ENr and FeENr below),  $\eta$  will be determined by Eqs. 13a and 13b (below) and will lie in the interval (0, 1). In the case of iron–light limitation (case FeE), no nitrate will be reduced, and  $\eta = 0$ . In the remaining three cases of maximum growth rate (case M), uptake limitation of ammonium and nitrate (case UAN), and pure light limitation (case E), the value of  $\eta$  is indeterminate.

To characterize cases ENr and FeENr, we must find  $\mu$  from Eqs. 4 through 8 under the assumption that  $\mu_{\text{N,pot}} = \mu_{\text{C,pot}}$ . This is most easily done by rewriting Eqs. 5 and 7 in the form (from Eq. 2)

$$\rho = \mu q_{\text{O}}/(1 - \mu/\mu'). \quad (10)$$

Using Eq. 10 to rewrite Eq. 5 for nitrogen yields

$$\rho_{\text{NO}_3,\text{red}} + \rho_{\text{NH}_4} = \mu q_{\text{N},0}/(1 - \mu/\mu'_{\text{N}}). \quad (11)$$

Then, using Eq. 10 to rewrite Eqs. 7a and 7b for carbon yields, respectively,

$$(1 - \eta)q_{\text{Fe}}\Phi_{\text{E}} - m_{\text{bas}} - m_{\text{red}}\rho_{\text{NO}_3,\text{red}} = \mu(q_{\text{C},0}/\epsilon_{\text{growth}})/(1 - \mu/\mu'_{\text{C}}) \quad (12a)$$

and

$$q_{\text{Fe}}\Phi_{\text{E}} - m_{\text{bas}} - (\Phi_{\text{E}}/\epsilon_{\text{red}} + m_{\text{red}})\rho_{\text{NO}_3,\text{red}} = \mu(q_{\text{C},0}/\epsilon_{\text{growth}})/(1 - \mu/\mu'_{\text{C}}). \quad (12b)$$

Eliminating  $\rho_{\text{NO}_3,\text{red}}$  from Eqs. 11 and 12 then yields

$$(1 - \eta)q_{\text{Fe}}\Phi_{\text{E}} - m_{\text{bas}} + m_{\text{red}}\rho_{\text{NH}_4,\text{pot}} = \mu \left[ \frac{q_{\text{N},0}m_{\text{red}}}{1 - \mu/\mu'_{\text{N}}} + \frac{q_{\text{C},0}/\epsilon_{\text{growth}}}{1 - \mu/\mu'_{\text{C}}} \right] \quad (13a)$$

and

$$(q_{\text{Fe}}\Phi_{\text{E}} - m_{\text{bas}}) + (\Phi_{\text{E}}/\epsilon_{\text{red}} + m_{\text{red}})\rho_{\text{NH}_4,\text{pot}} = \mu \left[ \frac{q_{\text{N},0}(\Phi_{\text{E}}/\epsilon_{\text{red}} + m_{\text{red}})}{1 - \mu/\mu'_{\text{N}}} + \frac{q_{\text{C},0}/\epsilon_{\text{growth}}}{1 - \mu/\mu'_{\text{C}}} \right]. \quad (13b)$$

Equations 13a and 13b are quadratic in  $\mu$  and can be solved in closed form for use in simulation modeling or for comparing the model to physiological data.

To apply the model, we must first determine which of the six cases of limitation apply in a given situation. The set of decision criteria outlined below can be used to evaluate which case is appropriate; other sets may prove more efficient in certain circumstances. Note that the criteria must be applied sequentially, because each assumes that previous cases have been eliminated from consideration. The decision

criteria involve the sequential evaluation of “test” growth rates,  $\mu_{ii}$ .

*Cases where  $\rho_{\text{NO}_3, \text{red}} = 0$* —We first consider cases in which no nitrate is reduced (cases E and FeE). The first test growth rate is  $\mu_{r1} = \mu_{\text{N}, \text{pot}}(\rho_{\text{N}, \text{pot}})$ , evaluated using  $\rho_{\text{N}, \text{pot}} = \rho_{\text{NH}_4, \text{pot}}$  in Eq. 5). We compare this potential ammonium-limited growth rate to two potential carbon-limited growth rates.

*Case FeE:* If ( $q_{\text{Fe}} < q_{\text{Fe}}^*$ ), evaluate  $\mu_{r2} = \mu_{\text{C}, \text{pot}}(\rho_{\text{C}, \text{pot}})$ , where  $\rho_{\text{C}, \text{pot}}$  is calculated using Eq. 7b with  $\rho_{\text{NO}_3, \text{red}} = 0$ . If  $\mu_{r2} < \mu_{r1}$ , shortage of energy (carbon) determines that cells cannot use all the ammonium they can take up, the system is in iron-light limitation (cf. Sunda and Huntsman 1997), and  $\mu = \mu_{r2}$ .

*Case E:* If ( $q_{\text{Fe}}^* < q_{\text{Fe}}$ ), cells have more than enough iron to saturate the photosynthetic apparatus. In this case, evaluate  $\mu_{r3} = \mu_{\text{C}, \text{pot}}(\rho_{\text{C}, \text{pot}})$ , calculating  $\rho_{\text{C}, \text{pot}}$  using Eq. 7a with  $\rho_{\text{NO}_3, \text{red}} = 0$  and with  $(1 - \eta)q_{\text{Fe}} = q_{\text{Fe}}^*$ . If  $\mu_{r3} < \mu_{r1}$ , there is sufficient iron, but low light causes the cells not to use all the ammonium they can take up; this is therefore a case of pure light limitation, and  $\mu = \mu_{r3}$ .

*Cases where  $\rho_{\text{NO}_3, \text{red}} > 0$* —Once the above cases have been eliminated, we can assume  $\rho_{\text{NO}_3, \text{red}} > 0$  in all further calculations. The test criterion for uptake limitation of ammonium and nitrate is  $\mu_{r4} = \mu_{\text{N}, \text{pot}}(\rho_{\text{N}, \text{pot}})$ , where  $\rho_{\text{N}, \text{pot}} = \rho_{\text{NO}_3, \text{pot}} + \rho_{\text{NH}_4, \text{pot}}$ . We also define two criteria for carbon-limited growth,  $\mu_{r5}$  from Eq. 13a using  $(1 - \eta) = q_{\text{Fe}}^*$  and  $\mu_{r6}$  using Eq. 13b. A priori, it is difficult to determine whether  $\mu_{r5}$  or  $\mu_{r6}$  will be smaller, because both contain the reductant term  $m_{\text{red}}\rho_{\text{NO}_3, \text{red}}$ . We know, however, that if  $\mu_{r5} < \mu_{r6}$ ,  $q_{\text{Fe}}$  is large enough that not all iron in the cell can be used; these are cases without iron limitation, where the value of  $\eta$  is indeterminate. On the other hand, if  $\mu_{r6} < \mu_{r5}$ , all iron in the cell is in use. In either case, the additional test criterion  $\mu_{r7} = \min\{\mu_{r5}, \mu_{r6}\}$  will be useful in the following cases.

*Case M:* If ( $\mu_{r5} > \mu_{\text{max}}$  and  $\mu_{r7} > \mu_{\text{max}}$ ), growth is not limited by iron, light, or nitrogenous substrates; this is a case of maximum growth rate, where  $\mu = \mu_{\text{max}}$ .

*Case UAN:* If ( $\mu_{r5} < \mu_{r7}$ ), there is sufficient iron and light but insufficient nitrogenous substrate; this is a case of ammonium-nitrate uptake limitation, and  $\mu = \mu_{r5}$ .

*Case FeENr:* If ( $\mu_{r6} < \mu_{r5}$ ), cells must partition scarce iron between energy acquisition and nitrate reduction; this is a case of iron-light-(reduced) nitrogen limitation, and  $\mu = \mu_{r6}$ .

*Case ENr:* If ( $\mu_{r5} < \mu_{r6}$ ), energy acquisition and nitrate reduction are limited by light, not by iron; this is a case of light-(reduced) nitrogen colimitation, and  $\mu = \mu_{r5}$ .

### Origin of the Wheeler-Kokkinakis pattern

*Single size classes under light-nitrogen and iron-light-nitrogen colimitation*—In cases of light-nitrogen (ENr) and iron-light-nitrogen (FeENr) colimitation, the potential growth rates  $\mu_{\text{C}, \text{pot}}$  and  $\mu_{\text{N}, \text{pot}}$  are equal, so growth rate can be determined using either Eq. 6 or 8. It is more informative to use the nitrogen equation (Eq. 6) rewritten as Eq. 11. First, substitute  $1/\mu'_{\text{N}} = 1 - (1 - q_{\text{N},0}/q_{\text{N}, \text{max}})\mu/\mu_{\text{max}}$  in Eq. 11 to obtain

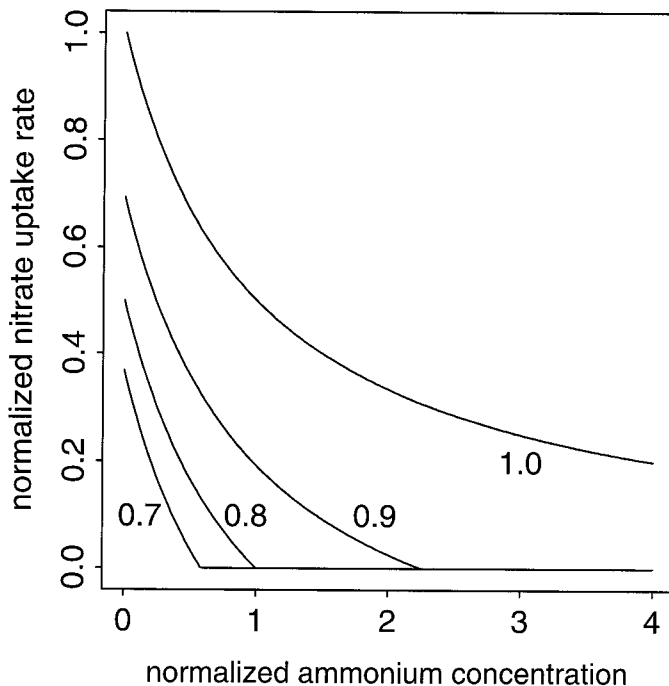


Fig. 3. Plots of Eq. 15, with reduction-limited nitrate uptake rate normalized to maximum nitrogen uptake rate ( $\rho_{\text{NO}_3, \text{red}}/\rho_{\text{N}, \text{max}}$ ) on the ordinate, versus ammonium concentration normalized to the half-saturation constant for ammonium uptake ( $[\text{NH}_4]/K_{\text{NH}_4}$ ) on the abscissa, for values  $\mu/\mu_{\text{max}} = \{0.7, 0.8, 0.9, 1.0\}$ . Note that only the curve for  $\mu/\mu_{\text{max}} = 1.0$  (unlimited growth) is asymptotic to the ammonium axis; all other curves intersect the ammonium axis at finite values.

$$\rho_{\text{NO}_3, \text{red}} + \rho_{\text{NH}_4, \text{pot}} = \frac{\mu q_{\text{N},0}}{1 - (1 - q_{\text{N},0}/q_{\text{N}, \text{max}})\mu/\mu_{\text{max}}}. \quad (14)$$

Then substitute Eq. 3a for  $\rho_{\text{NH}_4, \text{pot}}$ , divide the left side of Eq. 14 by  $\rho_{\text{N}, \text{max}}$  and the right side by  $\mu_{\text{max}}q_{\text{N}, \text{max}}$  ( $= \rho_{\text{N}, \text{max}}$ ), and rearrange slightly to obtain

$$\frac{\rho_{\text{NO}_3, \text{red}}}{\rho_{\text{N}, \text{max}}} = \frac{\mu/\mu_{\text{max}}}{q_{\text{N}, \text{max}}/q_{\text{N},0} + (1 - q_{\text{N}, \text{max}}/q_{\text{N},0})\mu/\mu_{\text{max}}} - \frac{[\text{NH}_4]}{[\text{NH}_4] + K_{\text{NH}_4}}. \quad (15)$$

This function is hyperbolic. When cells are growing at their maximum rate,  $\mu/\mu_{\text{max}} = 1$ , Eq. 15 reduces to the simple form  $\rho_{\text{NO}_3, \text{red}}/\rho_{\text{N}, \text{max}} = K_{\text{NH}_4}/([\text{NH}_4] + K_{\text{NH}_4})$ , which has its maximum value at 1 when  $[\text{NH}_4] = 0$ , approaching zero asymptotically as  $[\text{NH}_4] \rightarrow \infty$  (Fig. 3). However, for  $\mu/\mu_{\text{max}} < 1$ , both the maximum values and the asymptotic value are lowered equally, so that the resulting curve now intersects the ammonium axis (Fig. 3). For  $\mu/\mu_{\text{max}}$  values that are small enough, only the top portions of these curves are nonzero, which (given a certain amount of scatter in data) is suggestive of a straight line (Wheeler and Kokkinakis 1990).

Finally, Fig. 4 shows that this “straight-line” pattern can be produced even when phytoplankton are growing at an appreciable fraction of their maximum growth rates. For ex-

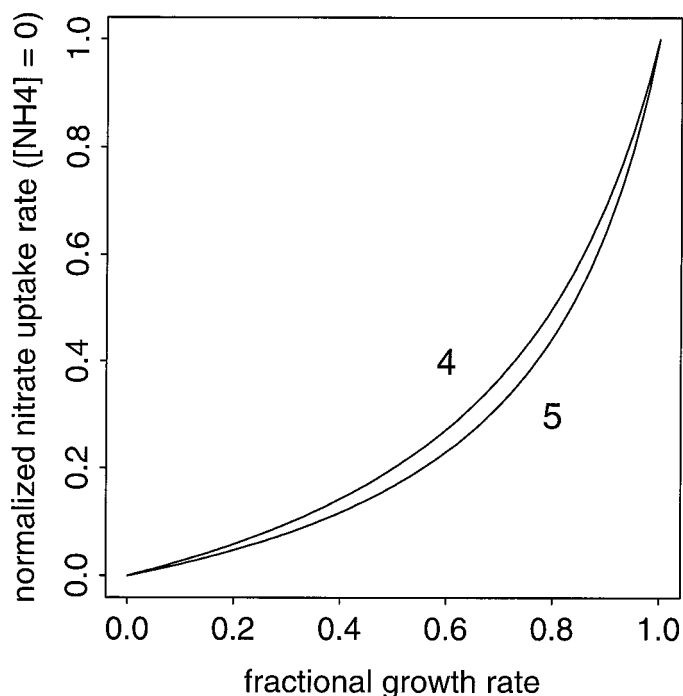


Fig. 4. On the ordinate is plotted the first term on the right side of Eq. 15, which is the reduction-limited nitrate uptake rate at zero ammonium normalized to the maximum nitrogen uptake rate [ $\rho_{\text{NO}_3, \text{red}}([\text{NH}_4] = 0)/\rho_{\text{N}, \text{max}}$ ]; the fractional growth rate ( $\mu/\mu_{\text{max}}$ ) is plotted on the abscissa. Curves are plotted for  $q_{\text{max}}/q_0 = \{4, 5\}$ , which are reasonable values for nitrogen storage (Morel 1987; Geider et al. 1998).

ample, with  $q_{\text{N}, \text{max}}/q_{\text{N}, 0} = 4$  (Fig. 4),  $\rho_{\text{NO}_3, \text{red}}/\rho_{\text{N}, \text{max}} = 0.5$  occurs at  $\mu/\mu_{\text{max}} = 0.8$ .

**Multiple discrete size classes**—The observation of the previous section suggests one key component of the Wheeler-Kokkinakis pattern: that when organisms are iron-replete and growing at near-maximal rates, curves of nitrate uptake versus ammonium concentration for single species should be roughly hyperbolic, with zero asymptotes at large nutrient concentrations; but when cells are iron-deficient, one sees only the tops of the hyperbolas, which may be statistically indistinguishable from straight lines. However, the diversity of shapes present in Fig. 1, together with the large range of apparent half-saturation constants  $K_{\text{NH}_4}$  that would be required to fit these curves, suggests that another factor must also be considered. I hypothesize that cell size is this other factor.

Half-saturation constants for nutrient uptake should increase with algal size due to surface-volume considerations (Hudson and Morel 1990), and there is theoretical (Hudson and Morel 1990; Aksnes and Egge 1991) and empirical (Eppley et al. 1969; Moloney and Field 1991) evidence that this scaling should be allometric (power law). For ammonium, the allometric dependence of the half-saturation constant  $K_{\text{NH}_4}$  on size can be written

$$K_{\text{NH}_4}(x) = K_{\text{NH}_4}(0)(L/L_0)^{\beta_{K_{\text{NH}_4}}} = K_{\text{NH}_4}(0)\exp(\beta_{K_{\text{NH}_4}}x), \quad (16)$$

where  $L$  is cell size,  $L_0$  is a reference size,  $x \equiv \log(L/L_0)$ ,

$K_{\text{NH}_4}(0)$  is the half-saturation constant for ammonium uptake at the reference size, and  $\beta_{K_{\text{NH}_4}}$  is the “allometric coefficient” for ammonium uptake. If an algal community contains species of several sizes, the resulting community uptake curve will be a mixture of their individual curves.

To see this point, consider Fig. 5. On the top row, I have constructed a model “high-iron” algal community with four species whose half-saturation values for ammonium uptake increase with size from 0.05 to 0.4  $\mu\text{M}$ . I have assumed that the two smallest species (half-saturation constants of 0.05 and 0.1  $\mu\text{M}$ ) can grow at maximum rates, so the uptake curves for both of them are hyperbolas that are asymptotic to the ammonium axis. The larger two larger species, however, are assumed to be iron limited (because of surface-volume considerations described by the iron analog of Eq. 16); they grow at  $\mu/\mu_{\text{max}} = 0.9$  and 0.8, respectively. The nitrate uptake curves for these species therefore intersect the ammonium axis at finite ammonium concentrations. Finally, I have assumed that species that are large enough to have growth rates  $\mu/\mu_{\text{max}} < 0.8$  will be rare enough that they can be ignored, because their growth rates are too small to keep up with background mortality due to physical mixing and/or generalized predation. Assuming that the four size classes that are present have roughly equal nitrogen biomasses (Chisholm 1992), the resulting average (“ave”) curve is asymptotic to the ammonium axis. The curve is not a simple hyperbola but the sum of contributions of the constituent size classes.

In contrast, consider the “iron-poor” community depicted on the lower row of Fig. 5. Here I have assumed that only the two smaller size classes ( $K_{\text{NH}_4} = 0.05$  and 0.1  $\mu\text{M}$ ) are present, and even they are growing at submaximal rates ( $\mu/\mu_{\text{max}} = 0.9$  and 0.8, respectively). In this case, both species’ nitrate uptake curves will intersect the ammonium axis, as will the average uptake curve.

Qualitatively, adding together the curves from several size classes can produce a wide range of shapes for uptake curves. As iron is increased in the presence of excess nitrate, smaller species will become less iron stressed and their growth rates will increase (compare, for example, the two rows of Fig. 5 for  $K_{\text{NH}_4} = 0.05$   $\mu\text{M}$ ). Larger species will also be added as iron supply is increased, and the largest of these will be under iron stress. Quantitative fits to data, however, require that growth rates be related quantitatively to iron abundance; the approach taken to produce the quantitative fits in Fig. 1 is described in the following section.

### Model simplifications for fitting data on community nitrate uptake

One approach to modeling community nitrate uptake would be to create a model with multiple species with both size and taxonomic (e.g., diatoms vs. coccolithophorids) diversity and then simulate the dynamics of each population. The descriptions of phytoplankton growth must be embedded in a food-web model to allow for predation losses and predation-caused shifts in the abundances of different taxa (e.g., Armstrong 1999).

This approach is too complicated for present purposes,

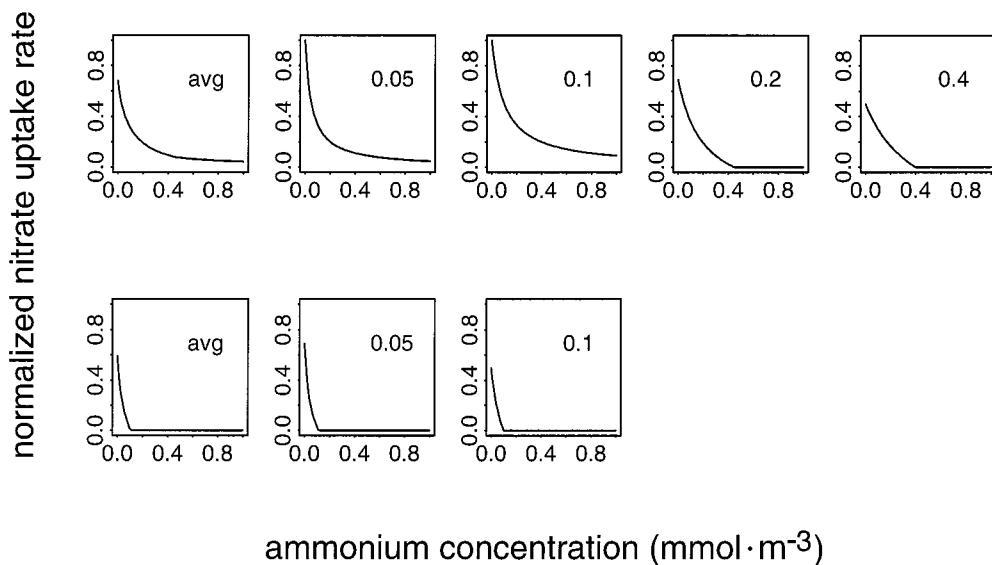


Fig. 5. Plots of reduction-limited nitrate uptake rates, normalized to maximum nitrogen uptake rate ( $\rho_{\text{NO}_3,\text{red}}/\rho_{\text{N,max}}$ ) on the ordinate, versus absolute ammonium concentration  $[\text{NH}_4]$  ( $\text{mmol m}^{-3}$ ) on the abscissa. The first panel, labeled “ave,” is the average of the curves in panels 2 through 5. Sizes of individual size classes increase from left to right; their sizes are characterized by their half-saturation constants for ammonium uptake  $K_{\text{NH}_4}$ , which are indicated on each panel: 0.05  $\mu\text{M}$ , 0.1  $\mu\text{M}$ , 0.2  $\mu\text{M}$ , and 0.4  $\mu\text{M}$ , respectively. The upper row represents a community of four species of different sizes in a relatively iron-rich environment. Note that the average curve is asymptotic to the ammonium axis. The lower row represents an iron-poor community, where only the two smallest species can survive. Again, “ave” represents the average community response, which in this case approximates a straight line, shutting off completely at roughly 0.1  $\mu\text{M}$  ammonium.

however. Therefore, instead of developing a model that will produce size spectra, I will assume that the algal community consists of equal amounts of biomass in equal logarithmic size classes up to some largest size  $x_{\text{max}}$  (Hurtt and Armstrong 1996, 1999; *see also* Chisholm 1992). This spectrum is then integrated against a linearized steady-state version of Eqs. 13b and 14, and parameters are estimated to give the best quantitative fit to the data in Fig. 1.

*Limit of large growth rates*—The first simplification is motivated by the now-classic study of Goldman et al. (1979), who noted that although the amounts of the elements C, N, and P in natural phytoplankton assemblages are usually in Redfield proportions 106:16:1, these ratios are achieved in chemostat experiments only when  $\mu/\mu_{\text{max}} \geq 0.9$ . Based on these observations, Goldman et al. (1979) concluded that in natural conditions, phytoplankton must typically be growing at a large fraction of their maximum rates. Then, because phytoplankton growing at near-maximal rates will have cell quotas near their maximum values, elemental ratios must be close to ratios of maximum cell quotas. To see this, note that

$$1 - \mu/\mu' = 1 - (\mu/\mu_{\text{max}})(1 - q_0/q_{\text{max}}) \rightarrow q_0/q_{\text{max}} \quad (17)$$

as  $\mu/\mu_{\text{max}} \rightarrow 1$ . In this limit, Eq. 13b reduces to

$$(q_{\text{Fe}}\Phi_{\text{E}} - m_{\text{bas}}) + (\Phi_{\text{E}}/\epsilon_{\text{red}} + m_{\text{red}})\rho_{\text{NH}_4,\text{pot}} \\ = \mu[q_{\text{N,max}}(\Phi_{\text{E}}/\epsilon_{\text{red}} + m_{\text{red}}) + q_{\text{C,max}}/\epsilon_{\text{growth}}]. \quad (18)$$

Because Eq. 18 is linear in  $\mu$ , it can easily be rearranged into the more transparent form:

$$\mu = \frac{(q_{\text{Fe}}\Phi_{\text{E}} - m_{\text{bas}}) + (\Phi_{\text{E}}/\epsilon_{\text{red}} + m_{\text{red}})\rho_{\text{NH}_4,\text{pot}}}{q_{\text{N,max}}(\Phi_{\text{E}}/\epsilon_{\text{red}} + m_{\text{red}}) + q_{\text{C,max}}/\epsilon_{\text{growth}}}. \quad (19)$$

Although Eq. 19 has been derived as a simplification of Eq. 13b to allow fitting nitrate uptake curves, it may prove to be of more general utility, because Sunda and Huntsman (1997) have shown an almost linear relationship between iron cell quota and growth rate (up to a point of saturation) in a variety of algal taxa.

In the limit of rapid growth, it is also true that  $\rho_{\text{NO}_3,\text{red}} = \rho_{\text{N,pot}} - \rho_{\text{NH}_4,\text{pot}} \approx \mu q_{\text{N,max}} - \rho_{\text{NH}_4,\text{pot}}$ ; substituting this into Eq. 19 and rearranging yields

$$\rho_{\text{NO}_3,\text{red}} \approx \frac{(q_{\text{Fe}}\Phi_{\text{E}} - m_{\text{bas}})(\epsilon_{\text{growth}}q_{\text{N,max}}/q_{\text{C,max}}) - \rho_{\text{NH}_4,\text{pot}}}{1 + (\Phi_{\text{E}}/\epsilon_{\text{red}} + m_{\text{red}})(\epsilon_{\text{growth}}q_{\text{N,max}}/q_{\text{C,max}})}. \quad (20)$$

Equation 20 demonstrates three consequences of increasing ammonium uptake,  $\rho_{\text{NH}_4,\text{pot}}$ : (1) that iron allocation shifts away from nitrate reduction, as it should; (2) that this replacement is not one-for-one, because the denominator of Eq. 20 is  $>1$ ; and (3) that the quantitative strength of the shift depends on light through  $\Phi_{\text{Fe}}$ .

*Instantaneous adjustment of  $q_{\text{Fe}}$  in the limit of large growth rates*—The second simplification arises from the need to recast Eqs. 19 and 20 in terms of  $\rho_{\text{Fe}}$  rather than  $q_{\text{Fe}}$ , because  $\rho_{\text{Fe}}$  can be modeled as having a relatively simple relationship to cell size and ambient iron concentration (the iron equivalent of Eq. 16); there is no equivalent relationship for  $q_{\text{Fe}}$ . In general, we could substitute  $q_{\text{Fe}} = \rho_{\text{Fe}}/\mu$  in Eq. 19,

Table 1. Parameter values for the fits of Fig. 1. The first three parameters were fit in common to all data sets, and the other parameters were fit with respect to a particular data set. For the fractional iron uptake rates of the smallest size class  $\rho_{\text{Fe}}(0)/\rho_{\text{Fe,max}}(0)$ , the numbers in parentheses are the estimated fractions multiplied by  $\alpha_{\text{E}}\rho_{\text{Fe,max}}(0)/\rho_{\text{N,max}}(0) = 41.0$ , and so are  $\alpha_{\text{E}}\rho_{\text{Fe}}(0)/\rho_{\text{N,max}}(0)$ . Values of  $\alpha_{\text{E}}\rho_{\text{Fe}}(0)/\rho_{\text{N,max}}(0) > 1$  imply that the smallest size classes are iron replete and can perform luxury consumption of iron, whereas values  $< 1$  imply iron limitation of even the smallest size classes (see Fig. 5). Parameters without specified units are dimensionless.

Parameter	Data set	Value	Units
$K_{\text{NH}_4}(0)$	Common	0.102	$\text{mmol m}^{-3}$
$\beta_{\text{E}}$	Common	0.974	
$\alpha_{\text{E}}\rho_{\text{Fe,max}}(0)/\rho_{\text{N,max}}(0)$	Common	41.0	
$\rho_{\text{Fe}}(0)/\rho_{\text{Fe,max}}(0)$	Cochlan (1986)	0.144 (5.9)	
	Garside (1981)	0.299 (12.3)	
	Glibert et al. (1982)	0.235 (9.6)	
	Olson (1980)	0.0972 (4.0)	
	Price et al. (1994)	0.0473 (1.9)	
	Wheeler and Kokkinakis (1990)	0.0144 (0.6)	
Uptake ( $[\text{NH}_4] = 0$ )	Price et al. (1994)	0.12	$\mu\text{mol L}^{-1} \text{d}^{-1}$
	Wheeler and Kokkinakis (1990)	6.06	$\text{nmol L}^{-1} \text{h}^{-1}$

which would result in a quadratic equation in  $\mu$ . However, in the limit  $\mu/\mu_{\text{max}} \approx 1$ , we can make the simplifications (1) that  $q_{\text{Fe}} \approx \rho_{\text{Fe}}/\mu_{\text{max}}$  and (2) that  $m_{\text{bas}}$  is small compared to energetic requirements for growth. These assumptions yield the following simplified form of Eq. 20:

$$\rho_{\text{NO}_3,\text{red}}/\rho_{\text{N,max}} \approx \alpha_{\text{E}}\rho_{\text{Fe}}/\rho_{\text{N,max}} - \beta_{\text{E}}\rho_{\text{NH}_4}/\rho_{\text{N,max}}, \quad (21)$$

where

$$\beta_{\text{E}} = [1 + (\Phi_{\text{E}}/\epsilon_{\text{red}} + m_{\text{red}})(\epsilon_{\text{growth}}q_{\text{N,max}}/q_{\text{C,max}})]^{-1} < 1 \quad (22)$$

and

$$\alpha_{\text{E}} = \beta_{\text{E}}\Phi_{\text{E}}\epsilon_{\text{growth}}q_{\text{N,max}}/(q_{\text{C,max}}\mu_{\text{max}}). \quad (23)$$

### Fitting the model to field data

The distribution of size dependence used here is one of “equal maximum chlorophyll in equal logarithmic size classes” (Chisholm 1992), where “equal maximum chlorophyll” is interpreted as equal nitrogen at maximum chlorophyll: nitrogen (Sakshaug et al. 1989; Hurtt and Armstrong 1996, 1999). We define  $x = \log(L/L_0)$ , where  $L$  is the equivalent spherical diameter and  $L_0$  is the diameter of the smallest phytoplankton present ( $L_0$  is assumed to be the same for all communities, roughly corresponding to the size of *Prochlorococcus*); the size distribution is therefore uniform (in nitrogen) on  $(0, x_{\text{max}})$ . Although this distribution is far from universal (Gin 1996 and references therein), it is a useful starting point for fitting data from natural populations; as knowledge of the causes of size distributions develops, better approximations will become possible.

Two studies were chosen to represent non-HNLC areas: the Scotian Shelf (Cochlan 1986) and the New York Bight (Garside 1981). Two studies were chosen to represent HNLC areas under putative iron limitation of total algal production: the subarctic Pacific (Wheeler and Kokkinakis 1990) and the equatorial Pacific (Price et al. 1994). Finally, two studies of the Southern Ocean (Glibert et al. 1982; Olson 1980), where the cause of the HNLC condition may also involve light limitation due to persistently deep mixing (Mitchell et al. 1991; Nelson and Smith 1991), were included to assess

whether the model could be used to deduce information regarding the causes of the HNLC condition in this region.

Data points corresponding to low-light conditions were discarded, because I wanted to fit common values of  $\alpha_{\text{E}}$  and  $\beta_{\text{E}}$  to all data sets, and nitrate uptake is known to be reduced under low light (Caperon and Ziemann 1976). Specifically, the  $< 5\%$  light category in Garside (1981) and the 0.1 and 6% light levels in Glibert et al. (1982) were removed. In addition, only the strongest relationship from Wheeler and Kokkinakis (1990; their fig. 6A, solid circles, data from June 1987) was fit to the models.

Fits were performed assuming that phytoplankton in a given location were in either case M (maximum growth rate), case FeENr (iron–light–nitrogen colimitation), or case FeE (iron–light colimitation). The smallest size classes would tend to be in case M, and the largest would tend to be in case FeE, with cells of intermediate size in case FeENr; however, the fits suggest that not all cases were present at every location (e.g., the subarctic Pacific, where the fit suggests that even the smallest size classes are in case FeENr).

Values for three parameters were assumed to be common to all studies, both to lessen the number of free parameters and to emphasize the flexibility of the model: the common parameters are (1)  $K_{\text{NH}_4}(0)$ ; (2)  $\beta_{\text{E}}$ ; and (3)  $\alpha_{\text{E}}\rho_{\text{Fe,max}}(x=0)/\rho_{\text{N,max}}(x=0)$ , the fraction of maximum uptake rate allowed for the smallest size class in the absence of ammonium. Other parameters were fit on a per-study basis: (4) fractional saturation of iron uptake of the smallest size class  $\rho_{\text{Fe}}(x=0)/\rho_{\text{Fe,max}}(x=0)$ , one for each of the six data sets; and (5) total maximum uptake rates at  $[\text{NH}_4] = 0$  for the two data sets with absolute uptake rates instead of  $f$  ratios (Fig. 1e, 1f; see also Table 1).

The curve-fitting procedure was a variant of the method of Metropolis et al. (1953; see also Press et al. 1986). In this procedure, a set of parameter values is used to generate a model prediction  $\hat{y}_i$  at each data point  $i$ . The likelihood,  $L$ , of the data set given the model is then calculated from

$$L = \prod_i^N \frac{1}{(2\pi\sigma_i^2)^{1/2}} e^{-(y_i - \hat{y}_i)^2/2\sigma_i^2}, \quad (24)$$

where  $\sigma_i^2$  is the model variance associated with data point  $i$ .

A constant coefficient of variation (Hurtt and Armstrong 1996) was specified by setting  $\sigma_i = a\hat{y}_i$  at each data point. Fitting proceeds by trying new values for parameters, comparing the previous likelihood with the new one, accepting parameter values associated with higher new likelihoods (plus a fraction of parameter values associated with lower new likelihoods, to avoid the problem of becoming trapped at a suboptimal peak), automatically searching parameter space for the best fit to the model.

$f$  ratios always lie in the interval (0, 1); therefore, to give all data points the same weight in the likelihood estimate, the data from Wheeler and Kokkinakis (1990) and Price et al. (1994) were normalized by dividing both data points  $y_i$  and predicted values  $\hat{y}_i$  by the corresponding maximum nitrate uptake rate.

Full details of the equations that were fit and of the procedure that was used for partitioning the spectra into segments corresponding to cases M, FeENr, and FeE are available from the author.

## Results

Results of curve fitting are depicted in Fig. 1, and the parameter estimates are summarized in Table 1. The value  $K_{\text{NH}_4}(0) = 0.102 \mu\text{mol m}^{-3}$  is quite reasonable (Eppley et al. 1969; Moloney and Field 1991; Carr unpubl. data). Values for the other two common parameters,  $\alpha_E$  and  $\beta_E$ , are difficult to interpret, because these parameters are predicted to vary with light, which was an unmeasured covariate that varied both within and between data sets. For this reason, the fits produced can only be taken as qualitative confirmation of the model's soundness; more work is needed to confirm its quantitative details.

The inferred degree of saturation of iron uptake of the smallest size classes  $\rho_{\text{Fe}}(0)/\rho_{\text{Fe,max}}(0)$  varied as expected, being high in the New York Bight (Fig. 1b) and low in the equatorial Pacific (Fig. 1e) and subarctic Pacific (Fig. 1f). In curves a through e of Fig. 3,  $\alpha_E\rho_{\text{Fe}}(0)/\rho_{\text{N,max}}(0)$ , the potential fraction of nitrate reduction in the smallest cells, was much greater than unity, implying the potential for significant luxury consumption of iron (Sunda and Huntsman 1995), at least by the smaller size classes. All these curves approached the ammonium axis asymptotically but did not intersect it. In the subarctic Pacific, in contrast, even the smallest size class was predicted to be acquiring iron at too low a rate to allow a maximum growth rate; the curve of nitrate uptake versus ammonium concentration (Fig. 3f) therefore intersects the ammonium axis at a finite value ( $\approx 0.15 \text{ mmol m}^{-3}$ ).

In the Southern Ocean (Figs. 1c, 1d), fractional saturation values were closer to those in non-HNLC areas than to those in HNLC areas (Table 1). One technically relevant point is that both Glibert et al. (1982) and Olson (1980) drew straight lines through their data, prompting the remark by Wheeler and Kokkinakis (1990) that two distinct types of inhibition curves may exist (presumably for HNLC and non-HNLC regions). However, the requirement that  $f$  ratios must converge to  $f = 1$  at  $[\text{NH}_4] = 0$  makes hyperbolic fits more reasonable in these plots from the Southern Ocean.

A more important caution in interpreting the Southern

Ocean plots is that they were constructed from data that were partly from shelf zones close to the ice margin, partly from ocean-open stations south of the Polar Front, and partly from stations north of the Polar Front. These zones appear to have very different levels of iron limitation. For example, Helbling et al. (1991) found a significant growth response to iron addition in the open ocean south of the Polar Front but no response in the shelf zone. Although the model fits to these data sets (Fig. 1) are therefore of limited value, fits to regionally restricted data sets should be useful both in diagnosing iron limitation and in predictive modeling.

## Discussion

The interaction of ammonium and nitrate, where availability of ammonium "inhibits" use of nitrate, is a key feature of many ecosystem models used in carbon-cycle research. Typically, this inhibition is represented by a simple mathematical expression multiplied by the nitrate uptake term (e.g., Wroblewski 1977; Fasham et al. 1990; Frost and Franzen 1992). However, use of the same functional form everywhere may be incorrect. In particular, Wheeler and Kokkinakis (1990) have suggested that there may be two types of functions relating nitrate uptake to ammonium concentrations: hyperbolic curves that asymptotically approach the ammonium axis and straight lines that intersect the axis at finite ammonium concentrations. The model developed here suggests that these two curves are limiting cases of a general hyperbolic model, which in the case of iron repletion should approach the ammonium axis asymptotically but which under increasing iron stress may intersect the ammonium axis (Fig. 3). If this model is correct, the strong ammonium inhibition of nitrate uptake observed by Wheeler and Kokkinakis (1990) is only the proximate cause of low nitrate use in the north Pacific; the ultimate cause would be low iron, and their article might be retitled "Iron scarcity limits cell size and nitrate use in the oceanic subarctic Pacific." Iron would limit total nitrate use both by limiting nitrate utilization within algal size classes and by excluding larger size classes from the phytoplankton community (Banse 1991; Armstrong 1994; Armstrong et al. 1994; Price et al. 1994).

By suggesting that iron may be an important unmeasured covariate in studies of ammonium inhibition of nitrate uptake, the present model may help explain the broad range of ammonium inhibition results that have been obtained. Dortch (1990), for example, has argued that the commonly-accepted paradigm of severe ammonium inhibition of nitrate uptake at ammonium concentrations  $>1 \mu\text{M}$  is far from universal; considering iron concentration as a covariate may lead to the recognition of a more nearly universal pattern.

Laboratory and field studies support the mechanistic basis of the model. Reuter and Ades (1987) showed that adding iron to cultures of *Scenedesmus quadricauda* increased nitrate uptake significantly, whereas ammonium uptake remained relatively constant, a finding that is in direct support of model premises. Iron addition to natural phytoplankton assemblages in the equatorial Pacific yielded similar results (Price et al. 1994). Explicitly including iron in modeling the

ammonium–nitrate relationship should lead to advances in both understanding and predictive capability not attainable from empirically derived models containing only ammonium and nitrate, including those of Zevenboom and Mur (1981), Harrison et al. (1987), and Collos (1989).

Quantitative comparisons of the model to empirical results are also instructive. Plots of nitrate uptake versus ammonium concentration from non-HNLC areas (Cochlan 1986; Garside 1981; see Fig. 1) tend to have long tails that appear hyperbolic. In contrast, a fairly straight line that intersects the ammonium axis was produced by fitting data to the North Pacific (Wheeler and Kokkinakis 1990; Fig. 1f), whereas a sharply descending curve with a long tail was produced by data from the equatorial Pacific (Price et al. 1994; Fig. 1e). Fits to data from the Southern Ocean south of the Polar Front (Glibert et al. 1982; Olson 1980) tend to look hyperbolic, with larger values of the fractional uptake saturation  $\rho_{\text{Fe}}(0)/\rho_{\text{Fe,max}}(0)$  (Table 1) than in HNLC regions; the heterogeneity of these data sources, however, dictates that this result must be viewed with caution (see “Fitting the model to field data”).

The data fits shown in Fig. 1 were produced by assuming that all size classes present were in case M (unlimited growth), case FeE (iron–light colimitation), or case FeENr (iron–light–nitrogen colimitation). In general, some species present could also be in case E (pure light limitation), case UAN (ammonium–nitrate uptake limitation), or case ENr (light–nitrogen colimitation). These cases could not be examined within the limitations of the fitting procedure used but could be represented in a more complete model of size spectra and taxonomic diversity (e.g., Armstrong 1999). Inclusion of these cases would further increase the range of uptake curves that the model could produce.

It would be most interesting to analyze plots of  $f$  ratio versus ammonium concentration from different sectors of the Southern Ocean with different levels of iron limitation. Iron–light colimitation (Sunda and Huntsman 1997), for example, can be represented explicitly in the present model, and size-fractionated measurements of the relation of nitrate uptake to ammonium concentration may indicate that some size classes are indeed under iron–light limitation. It may yet turn out that iron limitation, grazing, and deep convection (Mitchell et al. 1991; Nelson and Smith 1991) are not alternatives but are all necessary to explain the HNLC condition in the Southern Ocean.

## References

- AKSNES, D. L., AND J. K. EGGE. 1991. A theoretical model for nutrient uptake in phytoplankton. *Mar. Ecol. Prog. Ser.* **70**:65–72.
- ARMSTRONG, R. A. 1994. Grazing limitation and nutrient limitation in marine ecosystems: steady-state solutions of an ecosystem model with multiple food chains. *Limnol. Oceanogr.* **39**:597–608.
- . 1999. Stable model structures for representing biogeochemical diversity and size spectra in planktonic communities. *J. Plankton Res.* **21**:445–464.
- , S. BOLLENS, B. FROST, M. LANDRY, M. LANDSTEINER, AND J. MOISAN. 1994. Food webs, p. 25–35. *In* C. S. Davis and J. H. Steele [eds.], *Biological/physical modeling of upper ocean processes*. Tech. Rep. WHOI-94-32. Woods Hole Oceanographic Institution.
- BANSE, K. 1990. Does iron really limit phytoplankton production in the offshore subarctic Pacific? *Limnol. Oceanogr.* **35**:772–775.
- . 1991. Rates of phytoplankton cell division in the field and in iron enrichment experiments. *Limnol. Oceanogr.* **36**:1886–1898.
- BURMASTER, D. E. 1979. The continuous culture of phytoplankton: mathematical equivalence of three steady-state models. *Am. Nat.* **113**:123–134.
- CAPERON, J., AND D. A. ZIEMANN. 1976. Synergistic effects of nitrate and ammonium on the growth and uptake kinetics of *Monochrysis lutheri* in continuous culture. *Mar. Biol.* **36**:73–84.
- CHISHOLM, S. W. 1992. Phytoplankton size, p. 213–237. *In* P. G. Falkowski and A. D. Woodhead [eds.], *Primary productivity and biogeochemical cycles in the sea*. Plenum.
- COALE, K. H., AND OTHERS. 1996. A massive phytoplankton bloom induced by an ecosystem scale iron fertilization experiment in the equatorial Pacific Ocean. *Nature* **383**:495–501.
- COCHLAN, W. P. 1986. Seasonal study of uptake and regeneration of nitrate on the Scotian Shelf. *Continental Shelf Res.* **5**:555–577.
- COLLOS, Y. 1989. A linear model of external interactions during uptake of different forms of inorganic nitrogen by microalgae. *J. Plankton Res.* **11**:521–533.
- COOPER, D. J., A. J. WATSON, AND P. D. NIGHTINGALE. 1996. Large decrease in ocean-surface CO<sub>2</sub> fugacity in response to in situ iron fertilization. *Nature* **383**:511–513.
- DE BAAR, H. J. W., J. T. M. DE JONG, D. C. E. BAKKER, B. M. LOSCHER, C. VETH, U. BATHMANN, AND V. SMETACEK. 1995. Importance of iron for plankton blooms and carbon dioxide drawdown in the Southern Ocean. *Nature* **373**:412–415.
- DORTCH, Q. 1990. The interaction between ammonium and nitrate uptake in phytoplankton. *Mar. Ecol. Prog. Ser.* **61**:183–201.
- DROOP, M. R. 1968. Vitamin B<sub>12</sub> and marine biology, IV: the kinetics of uptake, growth and inhibition in *Monochrysis lutheri*. *J. Mar. Biol. Assoc. UK* **48**:689–733.
- , M. J. Mickelson, J. M. Scott, and M. F. Turner. 1982. Light and nutrient status of algal cells. *J. Mar. Biol. Assoc. UK* **62**:403–434.
- EPPLEY, R. W., J. N. ROGERS, AND J. J. MCCARTHY. 1969. Half-saturation constants for uptake of nitrate and ammonium by marine phytoplankton. *Limnol. Oceanogr.* **14**:912–920.
- FASHAM, M. J. R., H. W. DUCKLOW, AND S. M. MCKELVIE. 1990. A nitrogen-based model of plankton dynamics in the oceanic mixed layer. *J. Mar. Res.* **48**:591–639.
- FLYNN, K. J., M. J. R. FASHAM, AND C. R. HIPKIN. 1997. Modelling the interactions between ammonium and nitrate uptake in marine phytoplankton. *Phil. Trans. R. Soc. B* **352**:1625–1645.
- FROST, B. W., AND N. C. FRANZEN. 1992. Grazing and iron limitation in the control of phytoplankton stock and nutrient concentration, a chemostat analog of the Pacific equatorial upwelling zone. *Mar. Ecol. Prog. Ser.* **83**:291–303.
- GARSDIE, C. 1981. Nitrate and ammonia uptake in the apex of the New York Bight. *Limnol. Oceanogr.* **26**:731–739.
- GEIDER, R. J., H. L. MACINTYRE, AND T. M. KANA. 1998. A dynamic regulatory model of phytoplankton acclimation to light, nutrients, and temperature. *Limnol. Oceanogr.* **43**:679–694.
- GIN, K. Y. H. 1996. Microbial size spectra from diverse marine ecosystems. Ph.D. dissertation. Massachusetts Institute of Technology/Woods Hole Oceanographic Institution Joint Program in Ocean Science and Engineering.
- GLIBERT, P. M., D. C. BIGGS, AND J. J. MCCARTHY. 1982. Utiliza-

- tion of ammonium and nitrate during austral summer in the Scotia Sea. *Deep-Sea Res.* **29**:837–850.
- GOLDMAN, J. C. 1977. Steady state growth of phytoplankton in continuous culture: comparison in internal and external nutrient equations. *J. Phycol.* **13**:251–258.
- , J. J. MCCARTHY, AND D. G. PEAVEY. 1979. Growth rate influence on the chemical composition of phytoplankton in oceanic waters. *Nature* **279**:210–215.
- HARRISON, W. G., T. PLATT, AND M. R. LEWIS. 1987. *f*-Ratio and its relationship to ambient nitrate concentration in coastal waters. *J. Plankton Res.* **9**:235–248.
- HELBLING, E. W., V. VIALLAFANÉ, AND O. HOLM-HANSEN. 1991. Effect of iron on productivity and size distribution of Antarctic phytoplankton. *Limnol. Oceanogr.* **36**:1879–1885.
- HUDSON, R. J. M., AND F. M. M. MOREL. 1990. Iron transport in marine phytoplankton: kinetics of cellular and medium coordination complexes. *Limnol. Oceanogr.* **35**:1002–1020.
- HURTT, G. C., AND R. A. ARMSTRONG. 1996. A pelagic ecosystem model calibrated with BATS data. *Deep-Sea Res. II* **43**:653–683.
- , AND ———. 1999. A pelagic ecosystem model calibrated with BATS and OWS I data. *Deep-Sea Res. I* **46**:27–61.
- KUMAR, N., R. F. ANDERSON, R. A. MORTLOCK, P. N. FROELICH, P. KUBIK, B. DITTRICH-HANNEN, AND M. SUTER. 1995. Increased biological productivity and export production in the glacial Southern Ocean. *Nature* **378**:675–680.
- LANDRY, M. R., AND OTHERS. 1997. Iron and grazing constraints on primary production in the central equatorial Pacific: an EqPac synthesis. *Limnol. Oceanogr.* **42**:405–418.
- LAROCHE, J., P. W. BOYD, R. M. L. MCKAY, AND R. J. GEIDER. 1996. Flavodoxin as an in situ marker for iron stress in phytoplankton. *Nature* **382**:802–805.
- LEONARD, C. L., C. R. MCCLAIN, R. MURTUGUDDE, E. E. HOFMANN, AND L. W. HARDING, JR. 1999. An iron-based ecosystem model of the central equatorial Pacific. *J. Geophys. Res.* **104**:1325–1341.
- LOUKOS, H., B. FROST, D. E. HARRISON, AND J. W. MURRAY. 1997. An ecosystem model with iron limitation of primary production in the equatorial Pacific at 140°W. *Deep-Sea Res. II* **44**:2221–2249.
- METROPOLIS, N., A. W. ROSENBLUTH, M. N. ROSENBLUTH, A. H. TELLER, AND E. TELLER. 1953. Equation of state calculations for fast computing machines. *J. Chem. Physics* **21**:1087–1092.
- MILLER, C. B., B. W. FROST, P. A. WHEELER, M. R. LANDRY, N. WELSCHMEYER, AND T. M. POWELL. 1991. Ecological dynamics in the subarctic Pacific, a possibly iron-limited ecosystem. *Limnol. Oceanogr.* **36**:1600–1615.
- MITCHELL, B. G., E. A. BRODY, O. HOLM-HANSEN, C. MCCLAIN, AND J. BISHOP. 1991. Light limitation of phytoplankton biomass and macronutrient limitation in the Southern Ocean. *Limnol. Oceanogr.* **36**:1662–1677.
- MOLONEY, C. L., AND J. G. FIELD. 1991. The size-based dynamics of plankton food webs, I: a simulation model of carbon and nitrogen flows. *J. Plankton Res.* **13**:1003–1038.
- MOREL, F. M. M. 1987. Kinetics of nutrient uptake and growth in phytoplankton. *J. Phycol.* **232**:137–150.
- , R. J. M. HUDSON, AND N. M. PRICE. 1991. Limitation of productivity by trace metals in the sea. *Limnol. Oceanogr.* **36**:1742–1755.
- NELSON, D. M., AND W. O. SMITH, JR. 1991. Sverdrup revisited: critical depths, maximum chlorophyll levels, and the control of Southern Ocean productivity by the irradiance-mixing regime. *Limnol. Oceanogr.* **36**:1650–1661.
- OLSON, R. J. 1980. Nitrate and ammonium in Antarctic waters. *Limnol. Oceanogr.* **25**:1064–1074.
- PRESS, W. H., B. P. FLANNERY, S. A. TEUKOLSKY, AND W. T. VETTERLING. 1986. Numerical recipes. Cambridge Univ. Press.
- PRICE, N. M., L. F. ANDERSEN, AND F. M. M. MOREL. 1991. Iron and nitrogen nutrition of equatorial Pacific plankton. *Deep-Sea Res.* **38**:1361–1378.
- , B. A. AHNER, AND F. M. M. MOREL. 1994. The equatorial Pacific Ocean: grazer-controlled phytoplankton populations in an iron-limited ecosystem. *Limnol. Oceanogr.* **39**:520–534.
- REUTER, J. G., AND D. R. ADES. 1987. The role of iron nutrition in photosynthesis and nitrogen assimilation in *Scenedesmus quadricauda* (Chlorophyceae). *J. Phycol.* **23**:452–457.
- SAKSHAUG, E., K. ANDRESEN, AND D. KIEFER. 1989. A steady state description of growth and light absorption in the marine planktonic diatom *Skeletonema costatum*. *Limnol. Oceanogr.* **34**:198–205.
- SCIANDRA, A., AND OTHERS. 1997. Growth-compensating phenomena in continuous cultures of *Dunaliella tertiolecta* limited simultaneously by light and nitrate. *Limnol. Oceanogr.* **42**:1325–1339.
- SUNDA, W. G., AND S. A. HUNTSMAN. 1995. Iron uptake and growth limitation in oceanic and coastal phytoplankton. *Mar. Chem.* **50**:189–206.
- , AND ———. 1997. Interrelated influence of iron, light, and cell size on marine phytoplankton growth. *Nature* **390**:389–392.
- SYRETT, P. J. 1981. Nitrogen metabolism of microalgae. *Can. Bull. Fish. Aquat. Sci.* **210**:182–210.
- WHEELER, P. A., AND S. A. KOKKINAKIS. 1990. Ammonium recycling limits nitrate use in the oceanic subarctic Pacific. *Limnol. Oceanogr.* **35**:1267–1278.
- WROBLEWSKI, J. S. 1977. A model of plankton plume formation during variable Oregon upwelling. *J. Mar. Res.* **35**:357–394.
- ZEVENBOOM, W., AND L. MUR. 1981. Simultaneous short-term uptake of nitrate and ammonium by *Oscillatoria agardhii* grown in nitrate- or light-limited continuous culture. *J. General Microbiol.* **126**:355–363.

Received: 3 April 1998

Accepted: 2 December 1998

Amended: 4 May 1999